

**Mathematical Modelling of Methane Hydrates Dissociation in Porous Medium via
Depressurization Technique**

by

Fedawin anak Johing

13806

A project dissertation submitted in partial fulfillment of
the requirements for the
Bachelor of Engineering (Hons)
(Petroleum Engineering)

FYP II, May 2014

Universiti Teknologi PETRONAS

Bandar Seri Iskandar

31750 Tronoh

Perak Darul Ridzuan

CERTIFICATION OF APPROVAL

**Mathematical Modelling of Methane Hydrates Dissociation in Porous Medium via
Depressurization Technique**

by

Fedawin anak Johing

13806

A project dissertation submitted to the
Petroleum Engineering Programme
Universiti Teknologi PETRONAS
in partial fulfillment of the requirement for the
BACHELOR OF ENGINEERING (Hons)
(PETROLEUM)

Approved by,

(Mazlin bt. Idress)

UNIVERSITI TEKNOLOGI PETRONAS

TRONOH, PERAK

May 2014

CERTIFICATION OF ORIGINALITY

This is to certify that I am responsible for the work submitted in this project, that the original work is my own except as specified in the references and acknowledgements, and that the original work contained herein have not been undertaken or done by unspecified sources or persons.

FEDAWIN ANAK JOHING

ABSTRACT

The depleting of conventional energy resources and increasing energy demand has led to the development in non-conventional resources. Among the non-conventional resources that is getting more attention is methane hydrates. The current amount of methane hydrates reserves in the world is more than that of the total of oil and natural gas reserves combined. Past research papers introduced different kind of mathematical models to predict the production of methane from its hydrates. Due to the various approach used to construct the model, the effectiveness in using every model may differ one to another depending on the condition or the nature of the methane hydrates reservoir. At the present, there has not been any study in which the efficiency of the mathematical model is tested using data from various research papers that focus on the same area of interest. Thus the objective of this paper is to select various mathematical models that simulate the dissociation of methane hydrates in porous media via depressurization and ultimately, to verify the efficiency of the selected mathematical model by testing it with data from various research paper of the same scope of study. In this paper, the efficiency of a mathematical model by Kim et al. (1987) is investigated by using the available data from other related research papers. The efficiency is determined by comparing the mass generation rate which is calculated based on the data taken from the research paper to the mass generation rate which is determined from the experiment and simulation. Four research papers are used to obtain the required data and the scope of study focuses on depressurization technique only. In the findings, all of the percentage differences are within the range from 20.48% to 2028.05% between the calculated (measured) and predicted data. The large differences are due to the assumptions made in calculations, insufficient data in the research papers, variation in the experiment procedure and settings, and human errors while conducting the experiment. Since the calculated mass generation rate follows the declination trend of the predicted mass generation rate, it is concluded that Kim et al. (1987) mathematical model is the most efficient model to predict the dissociation of methane hydrates in porous media. Thus, the objectives are met. To improve the quality of the project, the mathematical model should be validated with more research papers that provide the necessary information. Apart from that, researchers should consider conducting their own experiments and study other mathematical models.

ACKNOWLEDGEMENT

First and foremost, I would like to thank my supervisor, Madam Mazlin bt. Idress for her constant support, encouragement and guidance. This project would not have been possible without her patronage. I would also like to thank Dr. Sia Chee Wee for his willingness to share his wisdom and knowledge. He has helped a lot towards the completion of my project despite having such a tight academic schedule. I also wish to express my gratitude to the rest of the Petroleum Engineering Department for its support and assistance throughout my project progress.

TABLE OF CONTENTS

CERTIFICATION OF APPROVAL	i
CERTIFICATION OF ORIGINALITY	ii
ABSTRACT	iii
ACKNOWLEDGEMENT	iv
LIST OF FIGURES	vii
LIST OF TABLES	viii
NOMENCLATURE	ix
CHAPTER 1: INTRODUCTION	1
1.1 Background of Study.....	1
1.2 Problem Statement.....	2
1.3 Significance of Project.....	3
1.4 Objectives and Scope of Study.....	3
1.5 Relevancy and Feasibility of the Project.....	4
CHAPTER 2: LITERATURE REVIEW AND THEORY	5
2.1 Introduction to Methane Hydrates.....	5
2.2 Mathematical Models.....	8
2.3 Types of Simulator Used.....	10
2.4 Initial Reservoir Conditions.....	10
2.5 Experimental Data.....	11
2.6 Outcome of the Research.....	12
CHAPTER 3: METHODOLOGY AND PROJECT WORK	14
3.1 Research Methodology.....	14
3.2 Project Activities.....	15
3.3 Calculations Procedure.....	16
3.4 Software Used.....	10
3.5 Project Key Milestone for FYP I and FYP II.....	18
3.6 Gantt Charts for FYP I and FYP II.....	19
CHAPTER 4: RESULTS AND DISCUSSION	21
4.1 The Most Ideal Mathematical Model.....	21

4.2	Predicted (Expected) Mass Generation Rate of Methane.....	21
4.3	Dissociation Rate Constant, k_B	24
4.4	Total Surface Area of Hydrates per Unit Volume, A_{HS}	26
4.5	Mass Generation Rate of Methane versus Time.....	28
CHAPTER 5:	CONCLUSION AND RECOMMENDATION.....	37
5.1	Conclusion.....	37
5.2	Recommendations.....	38
REFERENCES.....		39

LIST OF FIGURES

Figure 1: Methane hydrates structure. Adapted from Hydrates, 2014, Retrieved from http://apchemcyhs.wikispaces.com/Hydrates	5
Figure 2: The comparison between Youslf et al. (1991) simulation data and experimental data.....	12
Figure 3: The comparison between Nazridoust, K. and Ahmadi, G. (2007) simulation data and Masuda et al. (1999) experimental data using Berea sandstone core sample.....	13
Figure 4: Project flow.....	14
Figure 5: Gantt chart for FYP I	19
Figure 6: Gantt chart for FYP II.....	20
Figure 7: Mass generation rate of methane versus time for Nazridoust and Ahmadi (2007).....	31
Figure 8: Mass generation rate of methane versus time for Kumar et al. (2010).....	31
Figure 9: Mass generation rate of methane versus time for Liu and Gamwo (2012).....	32
Figure 10: Mass generation rate of methane versus time for Ruan et al. (2012).....	32
Figure 11: Comparison of mass generation rate for Nazridoust and Ahmadi (2007).....	34
Figure 12: Comparison of mass generation rate for Kumar et al. (2010).....	34
Figure 13: Comparison of mass generation rate for Liu and Gamwo (2012).....	35
Figure 14: Comparison of mass generation rate for Ruan et al. (2012).....	35

LIST OF TABLES

Table 1: Types of dimensional model and simulator used.....	10
Table 2: Project timeline for FYP I.....	18
Table 3: Project timeline for FYP II.....	19
Table 4: Predicted mass generation rate for Nazridoust and Ahmadi (2007).....	22
Table 5: Predicted mass generation rate for Kumar et al. (2010).....	22
Table 6: Predicted mass generation rate for Liu and Gamwo (2012).....	23
Table 7: Predicted mass generation rate for Ruan et al. (2012).....	23
Table 8: Dissociation rate constant for Nazridoust and Ahmadi (2007).....	24
Table 9: Dissociation rate constant for Kumar et al. (2010).....	24
Table 10: Dissociation rate constant for Liu and Gamwo (2012).....	25
Table 11: Dissociation rate constant for Ruan et al. (2012).....	25
Table 12: Total surface area of hydrates per unit volume for Nazridoust and Ahmadi (2007).....	26
Table 13: Total surface area of hydrates per unit volume for Kumar et al. (2010).....	26
Table 14: Total surface area of hydrates per unit volume for Liu and Gamwo (2012).....	27
Table 15: Total surface area of hydrates per unit volume for Ruan et al. (2012).....	27
Table 16: Calculated (Measured) Mass Generation Rate of Methane and Percentage Error for Nazridoust and Ahmadi (2007).....	29
Table 17: Calculated (Measured) Mass Generation Rate of Methane and Percentage Error for Kumar et al. (2010).....	29
Table 18: Calculated (Measured) Mass Generation Rate of Methane and Percentage Error for Liu and Gamwo (2012).....	29
Table 19: Calculated (Measured) Mass Generation Rate of Methane and Percentage Error for Ruan et al. (2012).....	29

NOMENCLATURE

A_s	Specific Surface Area
A_{dec}, A_{HS}, A_p	Surface Area of Hydrate per Unit Volume
C_p	Phase- Specific Heat Capacity
$CH_4 \cdot 5.75H_2O$	Methane Hydrates
k	Absolute Permeability
k_B	Dissociation Rate Constant
k_d	Hydrate-Decomposition Kinetic Coefficient
k_d^0	Intrinsic Dissociation Constant
k_{r1}	Relative Permeability of Phase 1
\dot{m}_1	Mass Rate per Unit Volume of Phase 1
M_1	Molecular Weight of Phase 1
n	Total Number of Blocks
\dot{n}_{gp}	Molar Generation of Methane Gas
P	Local Pressure in the Core
P_e	Equilibrium Pressure
p_1	Pressure of Phase 1
p_0	Pressure at Boundary $x=0$
\dot{q}_w	Energy Source
R	Gas Constant
r_{beads}	Radius of the Spherical Glass Beads
S_1	Saturation of Phase 1
t	Time
T	Temperature
T_{sc}	Temperature at Standard Conditions
x	Distance
v_{1r}	Relative Velocity of Phase 1
v_{1x}	Velocity of Phase 1
V	Volume
Z	Gas-Compressibility Factor
γ	Shape Factor

μ_1	Viscosity of Phase 1
\emptyset	Porosity
ρ_1	Density of Phase 1
ρ_{beads}	Density of the Glass Beads
ΔE	Activation Energy
ΔH_h	Latent Heat of Hydrate Decomposition and Formation
Δt	Time Increment
Δx	Distance Increment

CHAPTER 1

INTRODUCTION

1.1 Background of Study

A major problem that the energy industry is facing today is the approaching energy crisis. Many researchers have been conducting investigations in the search for new energy sources. Methane hydrates is slowly gaining attention as they could cater help world's growing energy demands in the future (Lonero, 2008). The case was not the same in the past thirty years when hydrates were just considered as 'novelty', says a professor at Scripps Institution of Oceanography and also a geochemist on the Integrated Ocean Drilling Program (IODP), Miriam Kastner ("Popular Mechanics: Methane Hydrates", 2009). According to Miriam, methane hydrate was not significant in the past until someone started to realize the potential that it has as the future energy resource.

The world has immense number of methane hydrates reserves which are untapped to date. According to Foran (2013), the Energy Information Administration (EIA) estimated that methane hydrates has more carbon than the combined total of Earth's fossil fuels. Thomas (2001) also has the same idea saying that the world's hydrates reserves are estimated to be 700, 000 Tcf or about double the amount of coal, oil and conventional gas in the world. EIA also claimed that methane hydrates could contain more than 100, 000 trillion cubic feet of natural gases (Foran, 2013). This claim is supported by Pfeifer (2014) who said that the experts agreed that the methane hydrates reserves are humungous despite the estimate of the resources varies widely. According to Makogon, Holditch and

Makogon (2007), the potential reserves of hydrated gas are more than 1.5×10^{16} cubic feet and they are distributed both on land and offshore.

Furthermore, methane hydrates reserves are more reachable than oil and gas reserves as they are located deeper underground. With the existing infrastructures that are already in place to extract oil and gas from their reserves, the investment needed to start extracting methane hydrates can be reduced too.

According to Steffones, Chaturvedi and Sihag (2014), among the countries that have been working on methane hydrates are Canada, China, India, Japan, South Korea and United States while some countries such as Bulgaria, Taiwan and Turkey have been conducting progressive research to estimate their national methane hydrate reserves. Pfeifer (2014) also revealed that China has discovered a mass gas hydrate reserve in the northern part of South China Sea in 2013. According to Demirbas (2010), high resolution of seismic surveys in 1997, 2001 and 2002 as well as drilling the Nankai Trough Wells have revealed that the subsurface gas hydrate is largely distributed at a depth interval from 200 m to 270 m below seafloor. In March 2013, Japan has emerged as the first country to achieve gas flowing from methane hydrate deposits under the Pacific Ocean. On another note, Hadley et al. (as cited in Ruppel, 2011, p. 1) mentioned that Malaysia has also started to launch major drilling hydrate expeditions starting in 2005.

1.2 Problem Statement

As the discovery of methane hydrates is still new in the energy industry, a lot of studies have been conducted that focus on developing mathematical modeling as a method to predict the production of methane gas when methane hydrate becomes unstable. One of the techniques used in methane gas production is depressurization. In most of the studies, the reliability of their mathematical models is tested by comparing the theoretical data to experimental data. The theoretical data is gotten from the mathematical model that has been converted into a simulation program. On the other hand, the experiment is conducted by using the same identical reservoir parameters to compare how close the theoretical data from the experimental data. Due to the various approach used to construct the model, the effectiveness in using every model may differ one to another depending on the condition

or the nature of the methane hydrates reservoir. At the present, there has not been a study in which the efficiency of the mathematical model is tested using data from various research papers that focus on the same area of interest.

1.3 Significance of Project

Mathematical model helps to manage the production of methane from its hydrates reservoir by predicting how much of the gas can be harvested over time. Therefore, this project is important as to validate the efficiency of the selected mathematical model. This project has a huge potential as a stepping stone in the development of more efficient mathematical models.

1.4 Objectives and Scope of Study

This project has two main objectives:

- i. To select various mathematical models that simulate the dissociation of methane hydrates in porous media via depressurization.
- ii. To verify the efficiency of the selected mathematical model by testing it with data from various research paper of the same scope of study.

The process of dissociation of methane hydrates in porous media can be achieved via several techniques, such as thermal stimulation and inhibitor fluid injections. Nevertheless, for the purpose of this project, the scope of study is narrowed down to depressurization technique only. There are also several mathematical models that have been introduced in past research papers. For this project, it focuses on validating one mathematical model only and this suffices the limited time frame that is allocated for this project.

1.5 Relevancy and Feasibility of the Project

Efficient mathematical model is important because it helps in the regulation of pressure at the hydrates reservoir during production. If the mathematical model is very efficient in predicting the production of methane from its hydrates, this also means that we can predict the minimum value of reservoir pressure that needs to be lowered down before it can start dissociation. With the right estimation, the cost of production and time consumption can be minimized. The implementation of this project is simple and cost-free as the entire project is conducted in Microsoft[®] Excel version 2013. With ample amount of time given and specific focus of the project, planning and modifications can be done properly to achieve the objectives of the project.

CHAPTER 2

LITERATURE REVIEW AND THEORY

2.1 Introduction to Methane Hydrates

A hydrate is an inorganic compound constituting of water and smaller molecules. In most cases, hydrates consist of a significant content of water, H₂O molecules by weight. The structure of clathrates compound is such that a molecule of a substance is encapsulated by a cage-like structure made of molecules of another substance. Hydrates have a general formula of M_n(H₂O)_p, in which one or more hydrate forming molecules M are called “guest” associated with p “host” water molecules (Lee and Holder, 2001). Gas hydrates can be categorized to a general class of inclusion compounds known as clathrates (Mahajan, Taylor and Mansoori, 2007).

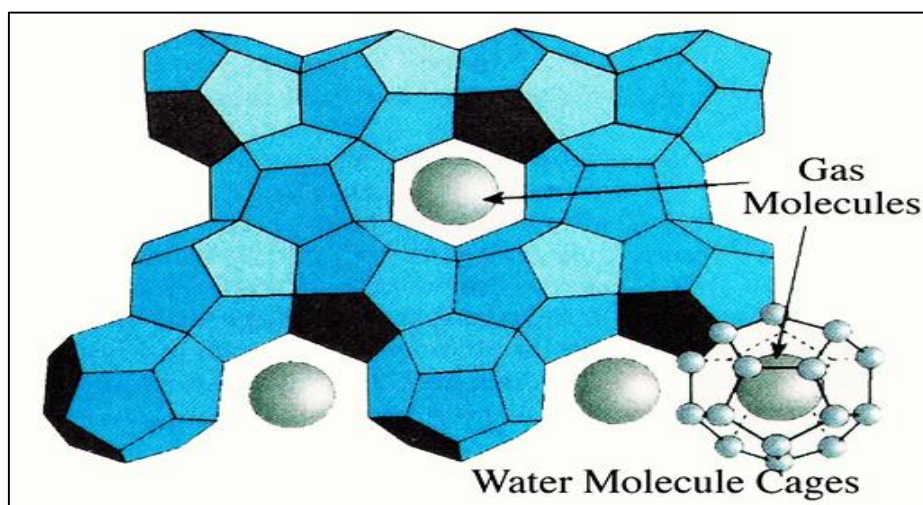


Figure 1: Methane hydrates structure. Adapted from Hydrates, 2014, Retrieved from <http://apchemcyhs.wikispaces.com/Hydrates>

Natural gases are fossil fuels formed naturally underground from dead animals and plants that are comprised of methane and other hydrocarbons. In subsurface rock reservoirs, many components of natural gases are reacting to water molecules to form gas hydrates. Gas hydrates are ice-like crystals that are formed naturally in a high pressure and low temperature condition at marine sediments where water depth is more than 300 meters where methane and pore water are sufficient.

In the energy sector, methane hydrates ($\text{CH}_4 \cdot 5.75\text{H}_2\text{O}$) is gaining its popularity as one of the potential energy sources of the future. This solid clathrate compound or clathrate hydrate is made of huge amount of methane enclosed within crystal structure of water. Methane hydrate is also known with other names such as methane hydrate, hydromethane, methane ice and natural gas hydrate.

The amount and rate of methane hydrates formation is dependent on the amount of methane supply. Methane molecules from the hydrate compound are formed from the microorganisms that consume buried detrital organic material and release methane as the by-product. Wright et al. (1998) stated that the deposition of methane hydrates take place in offshore sediments overlain by cold, deep water and in association with onshore occurrences of thick permafrost. Methane hydrates have unstable composition such that they can only exist in a region of limited physical conditions known as Hydrate Stability Zone (HSZ). Garg et. al (as cited in Lonero, 2008, p. 53) said that HSZ forms at 530 meters depth at northern latitudes and 250 metres for southern latitude.

The two sources of methane that contribute to the formation of methane hydrate in HSZ are in situ methane generation within HSZ and deep methane influx. Methane generation within HSZ involves in situ conversion of biomass to methane. However the methane produced are not as abundant, less pure and loosely held by sediments when compared to methane production via deep methane influx (Lonero, 2008). In deep methane influx, decomposition of carbon-rich organic matters within marine sediment layers releases methane and a trace of other impurities such as ethane, propane, carbon dioxide, nitrogen and hydrogen sulfate.

Dissociation of methane hydrates can be done through a few methods. The first method involves thermal stimulation where hot water or steam is injected into the hydrate beds to increase the temperature at the targeted region. The increase in temperature causes methane hydrates to become unstable thus releasing methane hydrates to the borehole and transported to the surface through the pipes. This method is simple, yet costly and as mentioned by Ruppel (2007), it may not reach deeper hydrate sediments. (as cited in Lonero, 2008, p. 57)

The second extraction method is via depressurization method. By drilling deep into the hydrate beds, it causes the in-situ pressure to drop under the equilibrium pressure of methane hydrate pressure at reservoir temperature. Nagao (2012) implied that depressurization method is cost-effective and predictable (and effective) for extracting gas from reservoirs of alternating layers of sand and mud. The drawbacks of this method are more unpredictable than other methods. Ruppel (as cited in Lonero, 2008, p. 57) also suggested that rapid process of depressurization causes the sediments and machineries to cool very fast that they can freeze, clog and malfunction.

The third method is inhibitor injection method. The idea of this technique is to inject inhibiting fluids such as methanol, ethanol or brines into the hydrates bed to alter the chemical composition of the local pore water that the hydrate compound loses its stability. This technique can prevent clogging of pipelines and wellhead. However, it may pose hazards to the environment if inhibitors other than brines are used.

According to Ruan et al. (2012), there is not any commercially proven methane hydrates production technique yet. The Messoyakha gas field in the northern part of the West Siberian Basin was produced via depressurization technique and is the only field case of long-term production of hydrate reservoir. The simple depressurization technique is regarded as the most promising mode for gas hydrate production compared with other suggested methods (Ruan et al., 2012). Nevertheless, the data about this reservoir are scarce and this situation restrains the learning of gas production behaviours of methane hydrate reservoirs. Without any other field experience, the studies that have been

conducted are mostly based on short-term production tests, laboratory experiments and mathematical models.

2.2 Mathematical Models

In the past few years, there have been several mathematical models that focus on depressurization technique as the main method to produce gas from its hydrates. Youslf et al. (1991) proposed a three phase, one dimensional (1D) mathematical model that involves a numerical approximation of space and time derivatives that resulted in a set of simultaneous nonlinear finite-difference equations. Youslf et al. (1991) treated the hydrate dissociation as a Kim et al. (1987) dynamic process. The results gained from the numerical model are compared with the experimental results of hydrate dissociation using Berea sandstone samples. The outcome is positive as the model matches with the experimental data. Their mathematical model is as follows:-

$$\frac{1}{\Delta x} \left(\frac{\rho_g k k_{rg}}{\mu_g \Delta x} \right)_{i+\frac{1}{2}} (p_{g_{i+1}} - p_{g_i}) - \frac{1}{\Delta x} \left(\frac{\rho_g k k_{rg}}{\mu_g \Delta x} \right)_{i-\frac{1}{2}} (p_{g_i} - p_{g_{i-1}}) + \dot{m}_{g_i} = \frac{1}{\Delta t} \{ [\phi_i \rho_{g_i} (1 - S_{w_i} - S_{H_i})]^{n+1} - [\phi_i \rho_{g_i} (1 - S_{w_i} - S_{H_i})]^n \} \dots \dots \dots (1)$$

$$\frac{1}{\Delta x} \left(\frac{\rho_w k k_{rw}}{\mu_w \Delta x} \right)_{i+\frac{1}{2}} (p_{w_{i+1}} - p_{c_{i+1}} - p_{g_i} + p_{c_i}) - \frac{1}{\Delta x} \left(\frac{\rho_w k k_{rw}}{\mu_w \Delta x} \right)_{i-\frac{1}{2}} (p_{g_i} - p_{c_i} - p_{g_{i-1}} + p_{c_{i-1}}) + \dot{m}_{w_i} = \frac{1}{\Delta t} [(\phi_i \rho_{w_i} S_{w_i})^{n+1} - (\phi_i \rho_{w_i} S_{w_i})^n] \dots \dots \dots (2)$$

$$-\dot{m}_{H_i} = \frac{1}{\Delta t} [(\phi_i \rho_{H_i} S_{H_i})^{n+1} - (\phi_i \rho_{H_i} S_{H_i})^n] \dots \dots \dots (3)$$

Similar to Youslf et al. (1991), the mathematical model by Nazridoust and Ahmadi (2007) was generated from the mathematical model developed by Kim et al. (1987). Their mathematical model was tested using a computer modeling approach where an axisymmetric model of a porous sandstone core is developed and solved for multiphase flows during the hydrate dissociation. The theoretical result was then compared to the experimental data by Masuda et al. (1999) and it shows that the modeling data did not deviate much from the experimental data.

Liang, Song and Chen (2010) used a two-dimensional (2D) simulator to model the methane hydrate dissociation in porous media via depressurization. The equations that govern the simulation include mass transport, intrinsic kinetic equation and energy conservation which are discretized via finite difference method and are solved in the implicit pressure-explicit saturation (IMPES) method. The study also relied on the experimental data by Masuda et al. (1999) and the simulation shows high similarity to the experimental data.

The mass conservations equations by Liang et al. (2010) are written below. Equations (4), (5) and (6) represent the mass balance of gas, water and hydrate respectively.

$$-\frac{1}{r} \frac{d}{dr} (r \rho_g v_{gr}) - \frac{d}{dx} (\rho_g v_{gx}) + \dot{q}_g + \dot{m}_g = \frac{d}{dt} (\phi \rho_g S_g) \dots \dots \dots (4)$$

$$-\frac{1}{r} \frac{d}{dr} (r \rho_w v_{wr}) - \frac{d}{dx} (\rho_w v_{wx}) + \dot{q}_w + \dot{m}_w = \frac{d}{dt} (\phi \rho_w S_w) \dots \dots \dots (5)$$

$$\dot{m}_h = \frac{d}{dt} (\phi \rho_h S_h) \dots \dots \dots (6)$$

Shahbazi and Pooladi-Darvish (2013) conducted a research on behavior of depressurization in Type III Hydrate Reservoirs. Type III Reservoir is hydrate layer squeezed by impermeable formations. Depressurization of Type III Reservoir is different from that of in porous media as the permeability in the hydrate is low. This research focuses on calculations of radius of investigation of the hydrate decomposition by means of analytical formula and simulation (numerical).

$$\frac{dm_{h,l}}{dt} = -VM_h k_d(T) A_{dec} (p - p_{eq}) \dots \dots \dots (7)$$

The surface area of the hydrates particles is expressed as a function of the number of moles of methane in the hydrates. This function satisfies several conditions such as invariant composition of the hydrate, uniform decomposition rate, constant number of particles during decomposition.

2.3 Types of Simulator Used

Table 1: Types of dimensional model and simulator used

Research paper/study by	Simulator used
Youslf et al. (1991)	Not specified
Nazridoust and Ahmadi (2007)	Gambit™ pre-processor
Liang et al. (2010)	2D-assymetrical method
Shahbazi and Pooladi-Dalvish (2013)	General Purpose Research Simulator (GPRS)-Hydrate

2.4 Initial Reservoir Conditions

The initial thermal condition of the outlet valve pressure was similar to the surrounding temperature. The temperature along the core prior to depressurization was assumed to be the same. In Youslf et al. (1991) case, they assumed that the depressurization process was carried out under isothermal conditions. In other studies, the temperature along the core changes with time. At the beginning of hydrate dissociation in the core sample, the temperatures in all the points of the core sample for both simulation and experimental data drop to minimum before rising again and approaching the surrounding temperature. This situation occurred since hydrate dissociation is an endothermic process and absorbs heat that subsequently results in the decreasing in temperature. The free convection heat transfer then causes the core temperature to approach the surrounding air temperature. Likewise, the initial pressure condition was also assumed to be the same along the core.

According to Shahbazi and Pooladi-Dalvish (2013), the application of ordinary differential equation (ODE) will only be valid if the initial reservoir condition is set closely to the equilibrium condition. The final independent variable, known as similarity variable, is a function of x and t . In a separate case study, the relationship between radius of investigation and square root of time was linear when the initial temperature and pressure of the reservoir were close to the equilibrium. However, when the initial temperature and pressure were greatly deviated from equilibrium, the relationship between radius of investigation and square root of time was non-linear (Shahbazi, 2010).

For all the studies, the pressure outlet boundary condition was defined on one of the side of the core, which represented the opening of the outlet valve. On all the walls of the core, no slip boundary condition was assumed. The core was assumed to be porous. Nazridoust and Ahmadi (2007) assumed that the initial porosities across the core varied with locations. In other studies, the condition of the porosity was not clearly stated and thus assumed to be homogenous throughout the core. All the studies agreed that the process of hydrate dissociation occurs at the front instead of the entire volume. Throughout the dissociation process, the so-called dissociation front moves from the exposed end towards the other end of the media with time. Dissociation front splits the reservoir into two regions. The end that is exposed to the external atmosphere contains both natural gas and water while the remaining region in the media is occupied by all the three phases, namely solid hydrates gas and water.

2.5 Experimental Data

Youslf et al. (1991) conducted their experiment using Berea sandstone. The experiment initial conditions were set similar to the simulation. However, the capillary pressure and relative permeability relationships for Berea stone were taken from Amyx et al. (1960). On the other hand, Nazridoust and Ahmadi (2007) and Liang et al. (2010) compared their simulation data to Masuda et al. (1999) experimental data using identical values of parameters. Masuda et al. (1999) conducted the experiment by using Berea sandstone core sample with a cylindrical geometry to investigate hydrate dissociation induced by depressurization. Shahbazi and Pooladi-Dalvish (2013) did not provide any experimental data to compare to their simulation data.

2.6 Outcome of the Research

Almost all the studies show high similarity between the simulation data and experimental data. For instance is the simulation data by Youslf et al. (1991) that obtained a satisfactory match with the experimental data. This is shown in Figure 3.

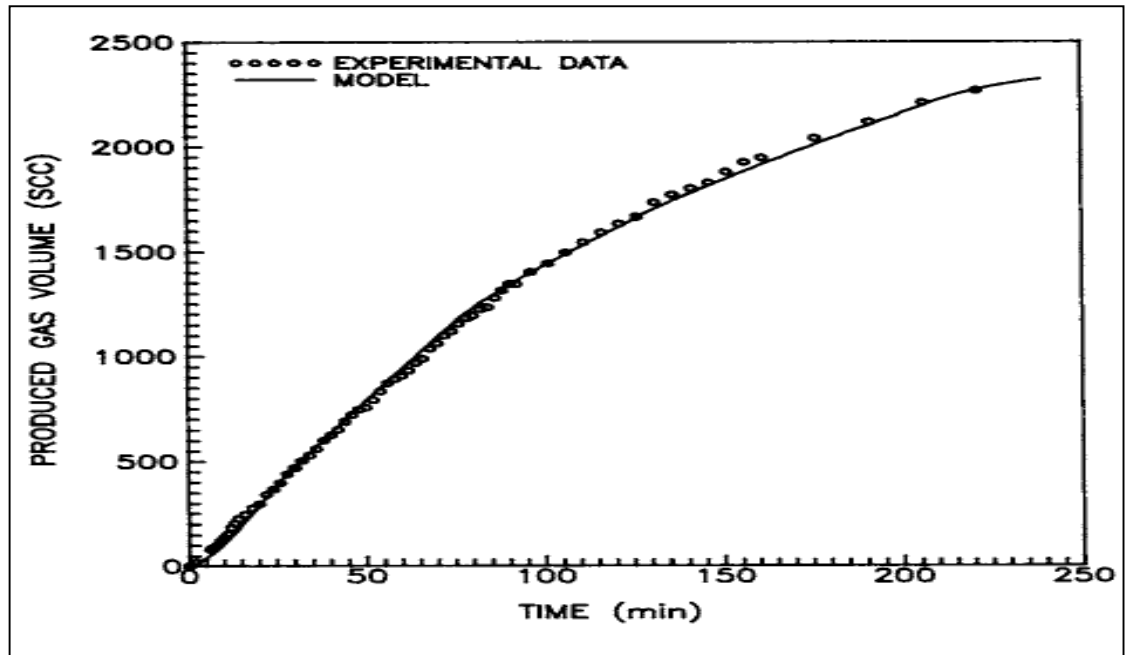


Figure 2: The comparison between Youslf et al. (1991) simulation data and experimental data.

Nazridoust and Ahmadi (2007) predicted that the core sample will generate a total gas bolume of 9014 standard cm^3 when all the hydrates get dissociated. The prediction was slightly lower than experiment data by Masuda et al. (1999) as the total volume of methane gas generated was found to be 9067 standard cm^3 . Nazridoust and Ahmadi (2007) reasoned that the deviation was as a result of numerical round off errors. The comparison of data is shown in Figure 4. Figure 5 shows the comparison of predicted gas production data and the experimental data by Liang et al. (2010). A very good agreement between them can be seen. The slight mismatch can be attributed to the lack of some experiment data (Liang et al., 2010).

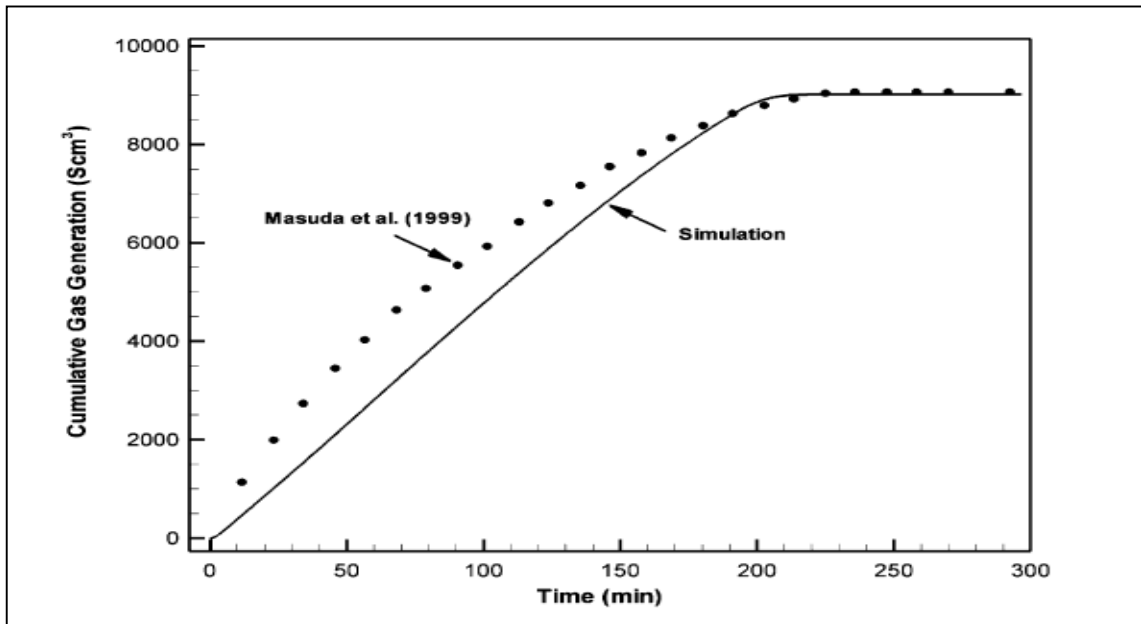


Figure 3: The comparison between Nazridoust, K. and Ahmadi, G. (2007) simulation data and Masuda et al. (1999) experimental data using Berea sandstone core sample.

CHAPTER 3

METHODOLOGY AND PROJECT WORK

3.1 Research Methodology

The following shows the sequences of the project flow from the beginning of the project until its completion.

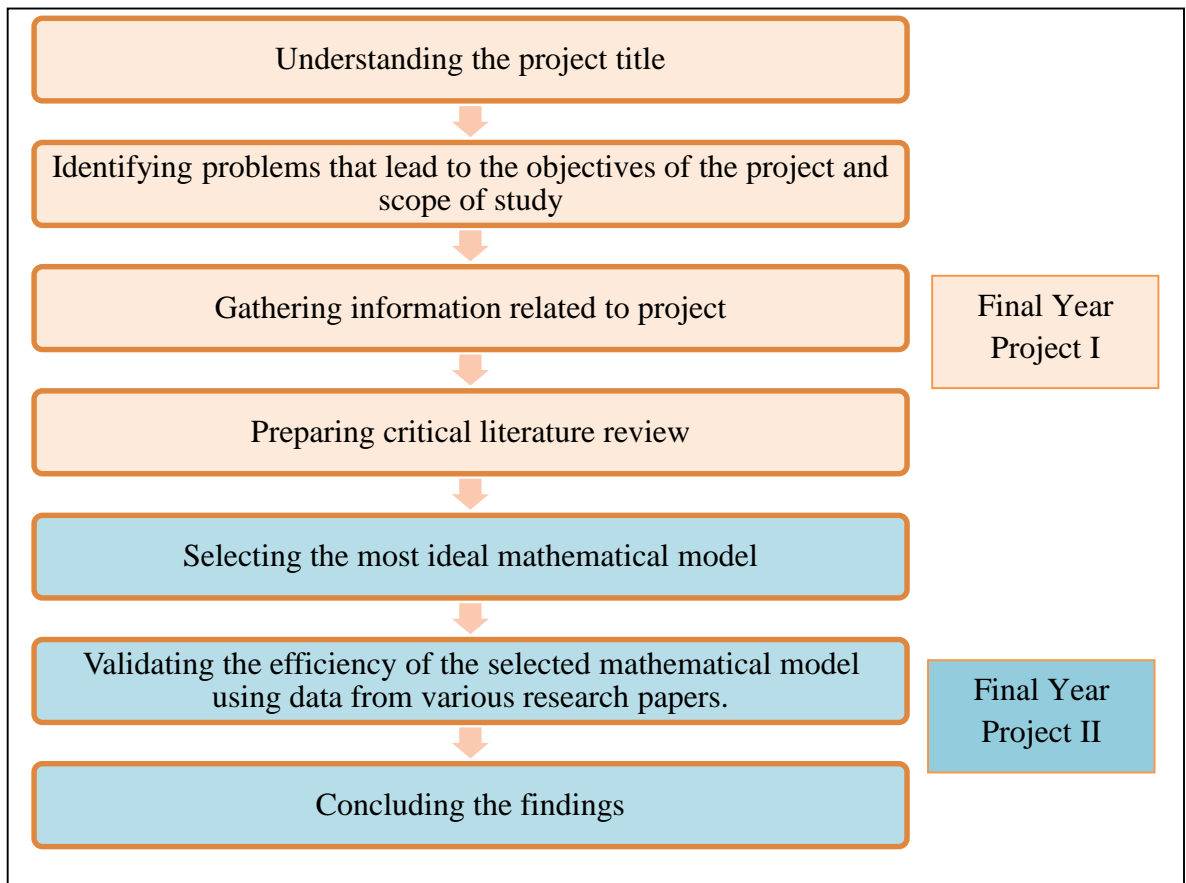


Figure 4: Project flow

3.2 Project activities

Stage 1: Understanding the project title. (FYP I)

Once the FYP title is determined, the first stage is to understand about the project entirely. This stage involves discussion with supervisor, Madam Mazlin, to get a clearer picture of the expected things that are going to be done within the next two semesters.

Stage 2: Identifying the problems that lead to the objectives of the project and scope of study. (FYP I)

Identifying the problem related to the project is vital as it gives a clearer direction of the final outcome of the project. The problem is identified through discussions with the supervisor and is further defined by referring to related past research papers. Once the problem statement is determined, objectives are set to solve the problem. The scope of study is defined clearly to ensure that the smoothness of the workflow within the specified time frame.

Stage 3: Gathering information related to project. (FYP I)

Information are gathered from past research papers which are obtained from the internet. These research papers contain various mathematical models as well as explanations related to their theory as well as simulation and experimental data. Apart from that, for in-depth understanding about methane hydrates, I did a lot of general readings regarding its environment, characteristics and its potential demand as a future energy source. Some important information that I gained also include the various techniques to recover methane and the amount of untapped methane hydrates reserves that the world has.

Stage 4: Preparing critical literature review. (FYP I)

This stage involves writing progress report to update on the work progress in the first semester. In the report, it also explains about my understanding on methane hydrates and

the things that has been done and needs to be done in the following semester. This reports is important as it ensures that the project is headed in the direction in which the objectives of the project will be ultimately achieved.

Stage 5: Selecting the most ideal mathematical model. (FYP II)

This stage is the most crucial one that is to select the most ideal mathematical model that is going to be used until the end of the project. The selection is based its popularity in other research papers as well as its ease of application.

Stage 6: Validating the efficiency of the selected mathematical model using data from various research papers. (FYP II)

Reservoir and experimental data are used to validate the efficiency of the selected model. By substituting the values into the mathematical model, it will yield the volume generation rate of methane at a specific period of time and this is compared to the existing and predicted volume generation rate taken from the respective research papers. Some of the data are not available in the research papers, thus, a lot of assumptions are made in this stage in which they are mostly responsible in the significant percentage errors in the calculations.

Stage 7: Concluding the findings. (FYP II)

After the calculations, the findings are interpreted and compiled in the project dissertation. At the end of the project findings, recommendations to improve the project will be included together with whether or not the objectives of the projects have been achieved.

3.3 Calculations Procedure

The mathematical model used in this project is developed by Kim et al. (1987). Nazridoust and Ahmadi (2007) further defined his mathematical model to calculate mass generation rate of gas and water per unit volume of the porous medium by hydrate dissociation. The equation is:-

$$\dot{m}_g = k_B M_g A_{HS} \emptyset S_H [P_e(T) - P] , \text{ where } P \leq P_e \dots \dots \dots (8)$$

To calculate k_B , the following formula is used:

$$k_B = k_d^0 \exp\left(-\frac{\Delta E}{RT}\right) \dots \dots \dots (9)$$

To calculate A_{HS} , the following formula is used:

$$A_{HS} = \gamma A_{hs} \dots \dots \dots (10)$$

where,

$$\gamma = \frac{250 \emptyset_i^2 S_h(x,t)}{(1 - S_h(x,t))^{3/2}} \dots \dots \dots (11)$$

and,

$$A_{hs} = \frac{3m_{beads}}{\rho_{beads} r_{beads} V_{cell}} \dots \dots \dots (12)$$

Step 1: Obtain data from research papers

The values of porosity, \emptyset , pressure, P , hydrate saturation, S_h , and temperature, T are taken from the graphs of these parameters versus time in different research papers, namely Kumar et al. (2010), Nazridoust and Ahmadi (2007), Liu and Gamwo (2012), Ruan et al. (2012). These values are taken from different time along the pressure drop region during the dissociation process. The volume of cell used is also taken from the research papers.

Like \emptyset , P , S_h , and T , the theoretical mass generation rates of methane at different time along the pressure drop during hydrates dissociation are also determined from the graph of volume generation rate versus time. The volume generation rate is converted to mass generation rate by multiplying it by the density of methane in standard condition.

The values of m_{beads} , ρ_{beads} and r_{beads} are taken from Kumar et al. (2013). The values are 0.12385kg, 2475 kg m⁻³ and 5.97 x 10⁻⁷m respectively. As for ΔE and k_d^0 , the values are 77 330 J/ kmol and 8.06 kmol/Pa/s/m², and are taken from Clarke and Bishnoi (2001).

Step 2: Calculate the mass generation rate using Kim et al. (1987) mathematical model.

Calculate the mass generation rate at different time along the pressure drop region during the dissociation process using equations 8 to 12. This step is made simpler by using Microsoft® Excel.

Step 3: Plot graphs and find percentage difference of theoretical mass generation rate to calculated mass generation rate.

Compare the results with the theoretical (predicted/expected) mass generation rate to the calculated mass generation rate over time. To check how much difference theoretical mass generation rate to the calculated mass generation rate, another similar graph is plotted where the values of theoretical mass generation rate are used at the x-axis.

3.4 Software Used

- Microsoft® Excel version 2013.

3.5 Project Key Milestone for FYP I and FYP II

Table 2: Project timeline for FYP I

WEEK	Objectives
FYP I (January 2014)	
2	Selection of project topic
3	Preliminary research work
6	Submission of extended proposal
8	Confirmation on software to run the mathematical models
8	Proposal defense
9	Continuation of project activities
13	Submission of interim draft report
14	Submission of interim report

Table 3: Project timeline for FYP II

WEEK	Objectives
FYP II (May 2014)	
2	Selecting the most ideal mathematical model.
3	Validating the efficiency of the mathematical model.
7	Submission of progress report
11	Submission of final draft of technical paper and project dissertation.
12	Submission of technical paper and project dissertation
13	Oral Presentation/ VIVA session

3.6 Gantt Charts for FYP I and FYP II

Description/ Project Activities	Week 1	Week 2	Week 3	Week 4	Week 5	Week 6	Week 7	Week 8	Week 9	Week 10	Week 11	Week 12	Week 13	Week 14
FYP I														
Title Selection														
Research/ Finding														
Literature Review														
Submission of Extended Proposal														
Preparation and Confirmation of software needed														
Proposal Defense														
Interim Draft Report Submission														
Interim Report Submission														

Figure 5: Gantt chart for FYP I

Description/ Project Activities	Week 1	Week 2	Week 3	Week 4	Week 5	Week 6	Week 7	Week 8	Week 9	Week 10	Week 11	Week 12	Week 13	Week 14
FYP II														
Selecting the most ideal mathematical model.														
Validating the efficiency of the mathematical model.														
Submission of progress report														
Pre-SEDeX														
Submission of final draft of technical paper and project dissertation.														
Submission of technical paper and project dissertation														
VIVA														

Figure 6: Gantt chart for FYP II

CHAPTER 4

RESULTS AND DISCUSSION

4.1 The Most Ideal Mathematical Model

The most ideal mathematical model is Kim et al. (1987) because the mathematical model is widely referred by many researchers as their base model such as Youslf et al. (1991), Nazridoust and Ahmadi (2007) and Ruan et al. (2012). Furthermore, the mathematical model by Kim et al. (1987) is simple and easy to use. As mentioned earlier, the mathematical model is as shown below:-

$$\dot{m}_g = k_B M_g A_{HS} \phi S_H [P_e(T) - P] , \text{ where } P \leq P_e \dots \dots \dots (13)$$

4.2 Predicted (Expected) Mass Generation Rate of Methane

In this section, mass generation rate is calculated and compared to the predicted mass generation rate which is converted from the volume generation rate. Parameters such as ϕ , P , S_h , and T are taken from four research papers along the pressure drop during methane hydrates dissociation. As the pressure drops, the pressure declines gradually as methane gas is released from the hydrate compound.

Table 4: Predicted mass generation rate for Nazridoust and Ahmadi (2007)

Time, T (s)	3000	4500	6.00×10^3	7.50×10^3	9.00×10^3
Temperature at equilibrium pressure, T_{Pe} (K)	275.45	275.45	275.45	275.45	275.45
Porosity, \emptyset	0.18	0.183	0.209	0.2525	0.26
Hydrate Saturation, S_H	0.556	0.549	0.4992	0.398	0.0231
Molar mass of methane, \dot{m} (kg/mol)	0.016	0.016	0.016	0.016	0.016
Density, ρ_{methane} (kg/m ³)	0.717	0.717	0.717	0.717	0.717
Pressure at equilibrium, P_e (psia)	3.75×10^8				
Pressure at time t , P (psia)	3.73×10^6	3.70×10^6	3.20×10^6	2.98×10^6	2.95×10^6
Pressure difference, $P_e - P$ (psia)	3.71×10^8	3.71×10^8	3.72×10^8	3.72×10^8	3.72×10^8
Volume generation rate of methane (m ³ /s) (predicted)	0.0903	0.0898	0.0838	0.0625	9.98×10^{-4}
Mass generation rate of methane (m ³ /s) (predicted)	0.064745	0.064387	0.060085	0.044812	7.16×10^{-4}

Table 5: Predicted mass generation rate for Kumar et al. (2010)

Time, T (s)	180	1440	2880	5100	7200
Temperature at equilibrium pressure, T_{Pe} (K)	277.2	277.2	277.2	277.2	277.2
Porosity, \emptyset	0.33	0.34	0.35	0.36	0.37
Hydrate Saturation, S_H	0.42	0.4093	0.3987	0.36167	0.01
Molar mass of methane, \dot{m} (kg/mol)	0.016	0.016	0.016	0.016	0.016
Density, ρ_{methane} (kg/m ³)	0.717	0.717	0.717	0.717	0.717
Pressure at equilibrium, P_e (psia)	3.50×10^8				
Pressure at time t , P (psia)	2.35×10^6	2.33×10^6	2.31×10^6	2.10×10^6	2.03×10^6
Pressure difference, $P_e - P$ (psia)	3.48×10^8				
Volume generation rate of methane (m ³ /s) (predicted)	0.435	0.424	0.41	0.35	6.71×10^{-4}
Mass generation rate of methane (m ³ /s) (predicted)	0.096795	0.092995	0.085323	0.063096	4.37×10^{-4}

Table 6: Predicted mass generation rate for Liu and Gamwo (2012)

Time, T (s)	900	1800	3000	3600	4200
Temperature at equilibrium pressure, T_{Pe} (K)	275.45	275.45	275.45	275.45	275.45
Porosity, \emptyset	0.182	0.184	0.234	0.278	0.3387
Hydrate Saturation, S_H	0.42	0.411	0.308	0.1978	0.0124
Molar mass of methane, \dot{m} (kg/mol)	0.016	0.016	0.016	0.016	0.016
Density, ρ_{methane} (kg/m ³)	0.717	0.717	0.717	0.717	0.717
Pressure at equilibrium, P_e (psia)	3.28×10^7				
Pressure at time t , P (psia)	2.84×10^6	2.60×10^6	2.50×10^6	2.45×10^6	2.43×10^6
Pressure difference, $P_e - P$ (psia)	3.00×10^7	3.02×10^7	3.03×10^7	3.04×10^7	3.04×10^7
Volume generation rate of methane (m ³ /s) (predicted)	0.040028	0.038494	0.032357	0.019915	9.3×10^{-5}
Mass generation rate of methane (m ³ /s) (predicted)	0.0287	0.0276	0.0232	0.0143	6.67×10^{-5}

Table 7: Predicted mass generation rate for Ruan et al. (2012)

Time, T (s)	600	1800	2400	3000	3600
Temperature at equilibrium pressure, T_{Pe} (K)	275.45	275.45	275.45	275.45	275.45
Porosity, \emptyset	0.182	0.185	0.19	0.21	0.25
Hydrate Saturation, S_H	0.41	0.395	0.36	0.25	0.04232
Molar mass of methane, \dot{m} (kg/mol)	0.016	0.016	0.016	0.016	0.016
Density, ρ_{methane} (kg/m ³)	0.717	0.717	0.717	0.717	0.717
Pressure at equilibrium, P_e (psia)	3.75×10^8	3.75×10^8	3.75×10^8	3.75×10^8	3.75×10^8
Pressure at time t , P (psia)	3.60×10^6	3.43×10^6	3.23×10^6	3.00×10^6	2.90×10^6
Pressure difference, $P_e - P$ (psia)	3.71×10^8	3.72×10^8	3.72×10^8	3.72×10^8	3.72×10^8
Volume generation rate of methane (m ³ /s) (predicted)	0.018689	0.016555	0.013752	8.842×10^{-3}	1.004×10^{-3}
Mass generation rate of methane (m ³ /s) (predicted)	0.0134	0.01187	0.00986	6.34×10^{-3}	7.2×10^{-4}

Table 4, Table 5, Table 6 and Table 7 shows the values of parameters that are needed in order to use Kim et al. (1987) mathematical model and taken from Nazridoust and Ahmadi (2007), Kumar et al. (2010), Liu and Gamwo (2012) and Ruan et al. (2012) respectively. For every research paper, the values of \emptyset , P, S_h , and T are taken from any five specific point along the dissociation process. Beyond the dissociation process, the rate of generation of methane remains unchanged, thus the data are not suitable to be used. In this mathematical model, the value of temperature is obtained at equilibrium pressure that is before the dissociation process started. The molar mass of methane is 16.04 g/mol or 0.016kg/mol. The density of methane used in this calculation 0.717 kg/m³, which is at standard condition. The assumption is still considerable because the temperature at which methane hydrate dissociation process takes place is very close to the standard temperature, that is 273.15 K or 0°C. During dissociation, the porosity increases as the more hydrates in the pores and coating the core particles are dissociated into methane and water. This also means that the saturation of hydrates decreases with time.

4.3 Dissociation Rate Constant, k_B

Table 8: Dissociation rate constant for Nazridoust and Ahmadi (2007)

Intrinsic dissociation rate, k_{do} (kmol/Pa/s/m ²)	8.06	8.06	8.06	8.06	8.06
Activation energy, ΔE , (J/kmol)	77330	77330	77330	77330	77330
Gas constant, R (J/mol·K)	8.314	8.314	8.314	8.314	8.314
Dissociation rate constant, k_B	1.7435 x 10 ⁻¹⁴				

Table 9: Dissociation rate constant for Kumar et al. (2010)

Intrinsic dissociation rate, k_{do} (kmol/Pa/s/m ²)	8.06	8.06	8.06	8.06	8.06
Activation energy, ΔE , (J/kmol)	77330	77330	77330	77330	77330
Gas constant, R (J/mol·K)	8.314	8.314	8.314	8.314	8.314
Dissociation rate constant, k_B	2.15776 x 10 ⁻¹⁴				

Table 10: Dissociation rate constant for Liu and Gamwo (2012)

Intrinsic dissociation rate, k_{do} (kmol/Pa/s/m ²)	8.06	8.06	8.06	8.06	8.06
Activation energy, ΔE , (J/kmol)	77330	77330	77330	77330	77330
Gas constant, R (J/mol·K)	8.314	8.314	8.314	8.314	8.314
Dissociation rate constant, k_B	1.743×10^{-14}				

Table 11: Dissociation rate constant for Ruan et al. (2012)

Intrinsic dissociation rate, k_{do} (kmol/Pa/s/m ²)	8.06	8.06	8.06	8.06	8.06
Activation energy, ΔE , (J/kmol)	77330	77330	77330	77330	77330
Gas constant, R (J/mol·K)	8.314	8.314	8.314	8.314	8.314
Dissociation rate constant, k_B	1.743×10^{-14}	1.74×10^{-14}	1.74×10^{-14}	1.74×10^{-14}	1.74×10^{-14}

The dissociation rate constant is calculated by considering the intrinsic dissociation rate, activation energy and gas constant. While the value for gas constant, $R=8.314$ J/mol·K is commonly used, the values for intrinsic dissociation rate and activation energy are assumed based on the suggestions by Clarke and Bishnoi (2001). Equation (9) is used to perform the calculation.

For instance, to calculate the dissociation rate constant for Nazridoust and Ahmadi (2007) at time=3000s,

$$k_B = k_d^0 \exp\left(-\frac{\Delta E}{RT}\right) = (8.06) \exp\left(-\frac{77330}{(8.314)(275.45)}\right) = 1.7435 \times 10^{-14}$$

4.4 Total Surface Area of Hydrates per Unit Volume, A_{HS}

Table 12: Total surface area of hydrates per unit volume for Nazridoust and Ahmadi (2007)

Mass of glass beads, m_{beads} (kg)	0.12385	0.12385	0.12385	0.12385	0.12385
Density of glass beads, ρ_{beads} (kg/m ³)	2475	2475	2475	2475	2475
Radius of glass beads, r (m)	5.97×10^{-5}				
Volume of cell, V_{cell} (m ³)	6.13×10^{-5}				
Area of grain surface area per unit volume of porous media, A_{hs} (m ² /m ³)	4.10×10^4				
Shape factor, γ	108	42.8	3.73	2.21	0.837
Total surface area of hydrates per unit volume, A_{HS} (m ² /m ³)	4.44×10^6	1.75×10^6	1.53×10^5	9.07×10^4	3.43×10^4

Table 13: Total surface area of hydrates per unit volume for Kumar et al. (2010)

Mass of glass beads, m_{beads} (kg)	0.12385	0.12385	0.12385	0.12385	0.12385
Density of glass beads, ρ_{beads} (kg/m ³)	2475	2475	2475	2475	2475
Radius of glass beads, r (m)	5.97×10^{-5}				
Volume of cell, V_{cell} (m ³)	9.39×10^{-5}				
Area of grain surface area per unit volume of porous media, A_{hs} (m ² /m ³)	2.68×10^4				
Shape factor, γ	1.17×10^2	1.15×10^2	1.12×10^2	9.01×10^1	7.05×10^1
Total surface area of hydrates per unit volume, A_{HS} (m ² /m ³)	3.14×10^2	3.07×10^6	3.01×10^6	2.41×10^6	1.89×10^6

Table 14: Total surface area of hydrates per unit volume for Liu and Gamwo (2012)

Mass of glass beads, m_{beads} (kg)	0.12385	0.12385	0.12385	0.12385	0.12385
Density of glass beads, ρ_{beads} (kg/m ³)	2475	2475	2475	2475	2475
Radius of glass beads, r (m)	5.97×10^{-5}				
Volume of cell, V_{cell} (m ³)	3.76×10^{-6}				
Area of grain surface area per unit volume of porous media, A_{hs} (m ² /m ³)	6.68×10^5				
Shape factor, γ	3.57×10^1	3.40×10^1	2.54×10^1	1.48×10^1	7.38×10^{-1}
Total surface area of hydrates per unit volume, A_{HS} (m ² /m ³)	2.38×10^7	2.28×10^7	1.70×10^7	9.89×10^6	4.93×10^5

Table 15: Total surface area of hydrates per unit volume for Ruan et al. (2012)

Mass of glass beads, m_{beads} (kg)	0.12385	0.12385	0.12385	0.12385	0.12385
Density of glass beads, ρ_{beads} (kg/m ³)	2475	2475	2475	2475	2475
Radius of glass beads, r (m)	5.97×10^{-5}				
Volume of cell, V_{cell} (m ³)	9.39×10^{-5}				
Area of grain surface area per unit volume of porous media, A_{hs} (m ² /m ³)	2.68×10^4				
Shape factor, γ	33.1	30.5	24.8	13.1	1.51
Total surface area of hydrates per unit volume, A_{HS} (m ² /m ³)	8.85×10^5	8.17×10^5	6.63×10^5	3.50×10^5	4.03×10^4

Table 8, Table 9, Table 10 and Table 11 show the values that are needed to calculate the total surface area of hydrates per unit volume for Nazridoust and Ahmadi (2007), Kumar et al. (2010), Liu and Gamwo (2012) and Ruan et al. (2012) respectively. In this project, it is assumed that methane hydrates is formed in a cell packed with spherical glass beads. Thus, the mass, density and radius of glass beads are used to find the total surface area of

hydrates per unit volume. All of the values are taken from a research by Kumar et al. (2013).

To calculate A_{HS} , equations (10), (11) and (12) are used. Shape factor (equation (11)) is calculated to account for the distribution of hydrate in pore space. According to Kumar et al. (2013), it is found by history matching the experimental and simulation results. Hydrates saturation is taken into account in this formula because the decreasing hydrates saturation during the dissociation process will alter the surface area of hydrates. According to Kumar et al. (2010), for hydrate saturation that is less than 35%, it is assumed that the hydrate formation habit is grain-coating. For that matter, equation (12) is used to calculate the area of grain surface area per unit volume of porous media. In this project, despite that most of the data started from a saturation higher than 30%, equation (12) is still valid as the hydrate saturation eventually drops below 30%.

For instance, to calculate the total surface area of hydrates per unit volume for Nazridoust and Ahmadi (2007) at time=3000s,

$$\gamma = \frac{250 \phi_i^2 S_h(x,t)}{(1 - S_h(x,t))^{3/2}} = \frac{250 (0.18)^2 (0.562)}{(1 - 0.562)^{3/2}} = 108$$

$$A_{hs} = \frac{3m_{beads}}{\rho_{beads} r_{beads} V_{cell}} = \frac{3 (0.12385)}{2475 \times 5.97 \times 10^{-5} \times 6.13 \times 10^{-5}} = 4.10 \times 10^4 \frac{m^2}{m^3}$$

$$A_{HS} = \gamma A_{hs} = (108)(4.10 \times 10^4) = 4.44 \times 10^4 \frac{m^2}{m^3}$$

4.5 Mass Generation Rate of Methane

Once all the needed parameters are calculated, the required values are substituted into equation (13). For instance, to calculate the total surface area of hydrates per unit volume for Nazridoust and Ahmadi (2007) at time=3000s,

$$\begin{aligned} \dot{m}_g &= k_B M_g A_{HS} \phi S_H [P_e(T) - P] \\ &= (1.7435 \times 10^{-14}) (0.016) (4.44 \times 10^6) (0.18) (0.556) (3.71 \times 10^8) \\ &= 7.89 \times 10^{-2} \text{ kg/s.} \end{aligned}$$

Table 16, Table 17, Table 18 and Table 19 show the values of mass generation rate of methane for every specific time for Nazridoust and Ahmadi (2007), Kumar et al. (2010), Liu and Gamwo (2012) and Ruan et al. (2012) respectively.

Table 16: Calculated (Measured) Mass Generation Rate of Methane and Percentage Error for Nazridoust and Ahmadi (2007)

Mass generation rate of methane (calculated)	7.89×10^{-2}	7.81×10^{-2}	7.74×10^{-2}	6.26×10^{-2}	9.29×10^{-4}
Mass generation rate of methane (predicted)	0.064745	0.064387	0.060085	0.044812	7.16×10^{-4}
Percentage error (%)	21.81	21.277	28.74	39.80	29.833

Table 17: Calculated (Measured) Mass Generation Rate of Methane and Percentage Error for Kumar et al. (2010)

Mass generation rate of methane (calculated)	1.25×10^{-1}	1.26×10^{-1}	1.27×10^{-1}	1.05×10^{-1}	8.41×10^{-4}
Mass generation rate of methane (predicted)	0.096795	0.092995	0.085323	0.063096	4.37×10^{-4}
Percentage error (%)	28.66	35.12	48.37	65.64	92.41

Table 18: Calculated (Measured) Mass Generation Rate of Methane and Percentage Error for Liu and Gamwo (2012)

Mass generation rate of methane (calculated)	3.63×10^{-2}	3.54×10^{-2}	3.37×10^{-2}	2.33×10^{-2}	1.42×10^{-3}
Mass generation rate of methane (predicted)	2.87×10^{-2}	0.0276	0.0232	0.014279	0.0000667
Percentage error (%)	26.58	28.11	45.34	63.50	2028.05

Table 19: Calculated (Measured) Mass Generation Rate of Methane and Percentage Error for Ruan et al. (2012)

Mass generation rate of methane (calculated)	1.67×10^{-2}	1.57×10^{-2}	1.31×10^{-2}	7.64×10^{-3}	1.05×10^{-3}
Mass generation rate of methane (predicted)	1.34×10^{-2}	1.19×10^{-2}	9.86×10^{-3}	6.34×10^{-3}	7.20×10^{-4}
Percentage error (%)	24.80	32.28	32.89	20.48	45.57

The percentage error is calculated to check the difference in value between calculated and predicted mass generation rate of methane at specific time. For instance, to calculate the percentage error for Nazridoust and Ahmadi (2007) at time=3000s:

$$\begin{aligned} \text{Percentage error} &= \left| \frac{\text{Predicted (Expected)Data} - \text{Calculated Data}}{\text{Predicted Data}} \right| \times 100\% \\ &= \left| \frac{0.064745 - 7.89 \times 10^{-2}}{0.064745} \right| \times 100\% = 21.81\% \end{aligned}$$

The difference between the values of calculated and predicted mass generation rate can also be presented in a graph. For the predicted graph line, the values of every x- and y-coordinate are using the value of the predicted mass generation rate itself. This is to ensure that the line can be formed linearly. As for the calculated graph line, the value for x-coordinate is the value of the predicted mass generation rate at a similar time of occurrence, while the y-coordinate is the value of the calculated mass generation rate.

Figure 7, Figure 8, Figure 9 and Figure 10 show graph of mass generation rate against time for both calculated and predicted for Nazridoust and Ahmadi (2007), Kumar et al. (2010), Liu and Gamwo (2012) and Ruan et al. (2012) respectively.

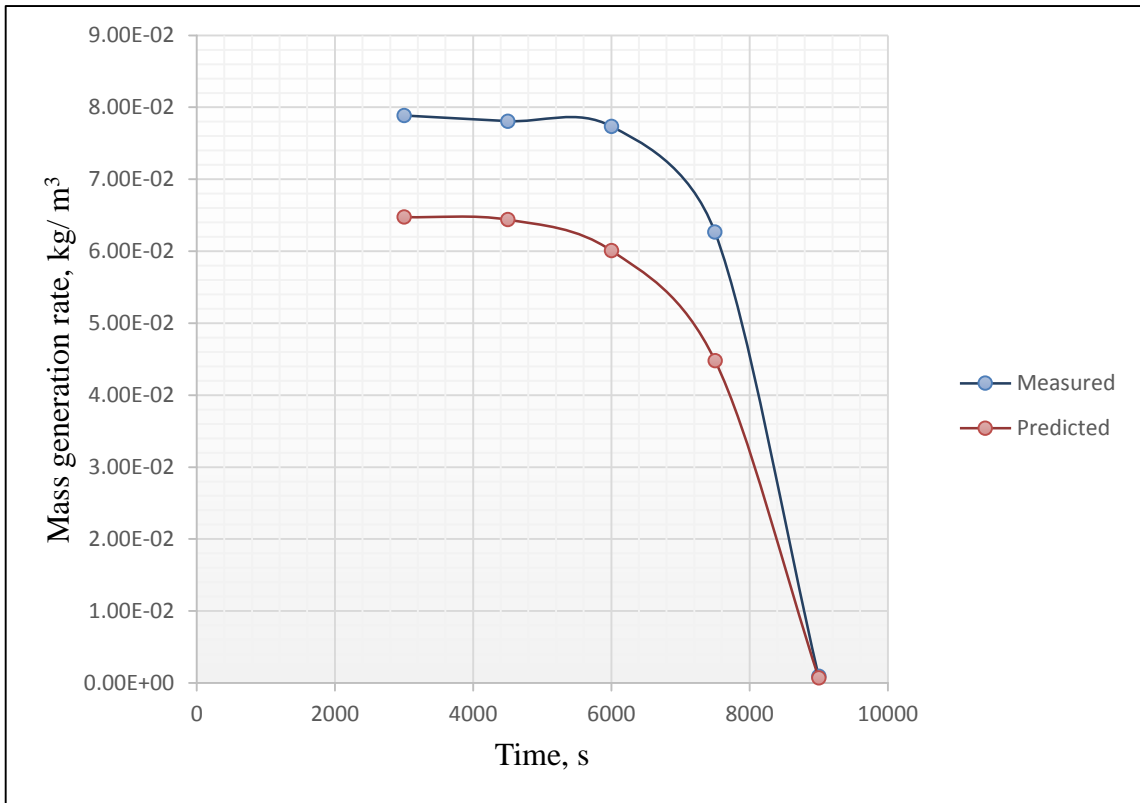


Figure 7: Mass generation rate of methane versus time for Nazridoust and Ahmadi (2007)

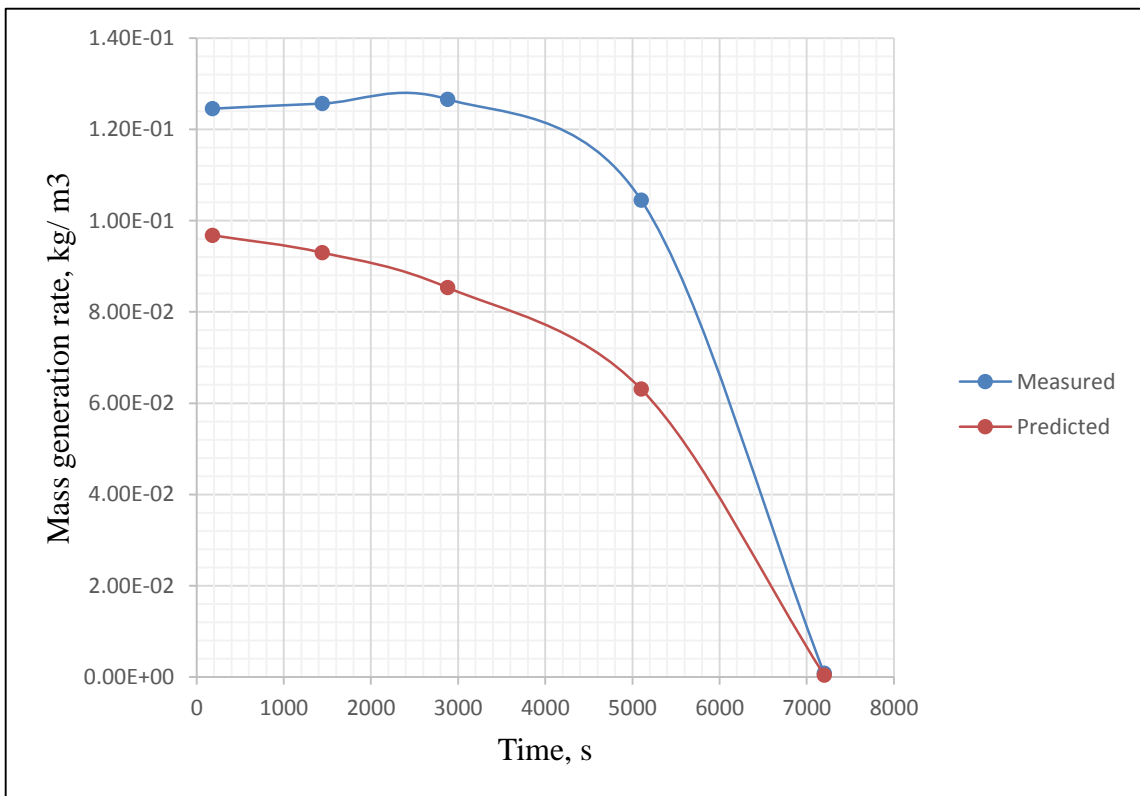


Figure 8: Mass generation rate of methane versus time for Kumar et al. (2010)

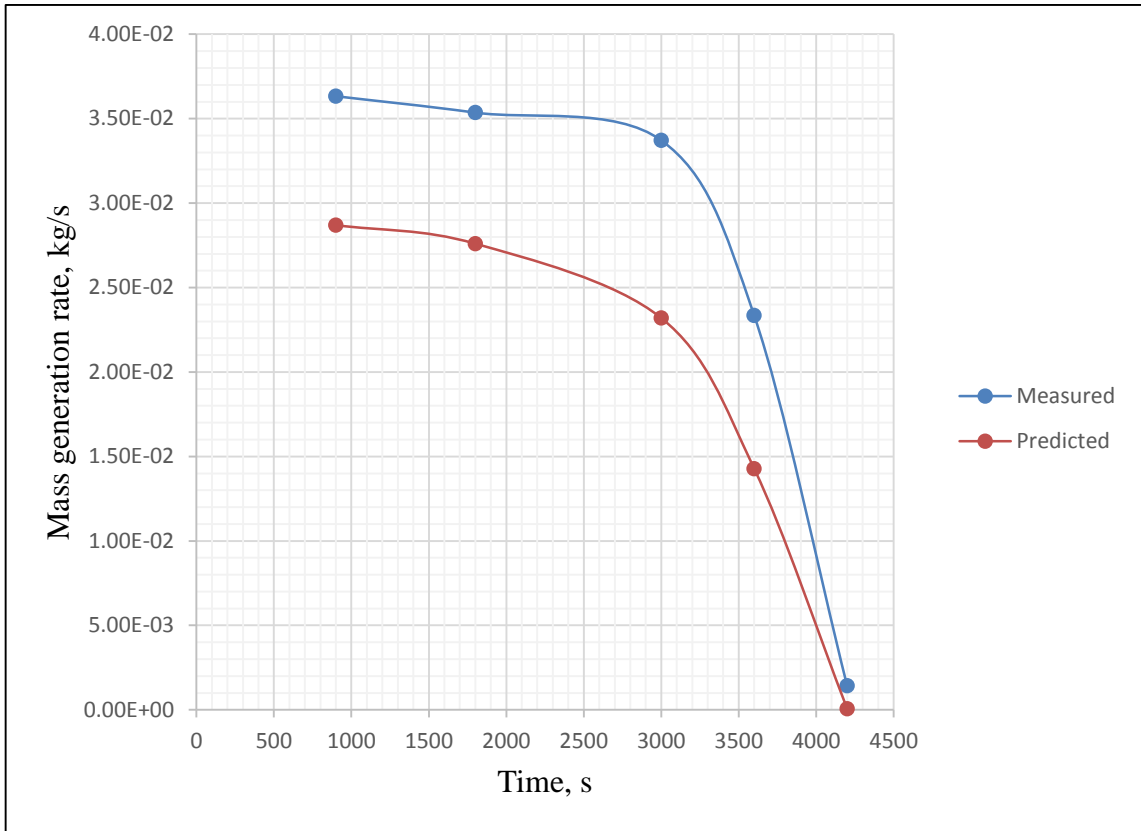


Figure 9: Mass generation rate of methane versus time for Liu and Gamwo (2012)

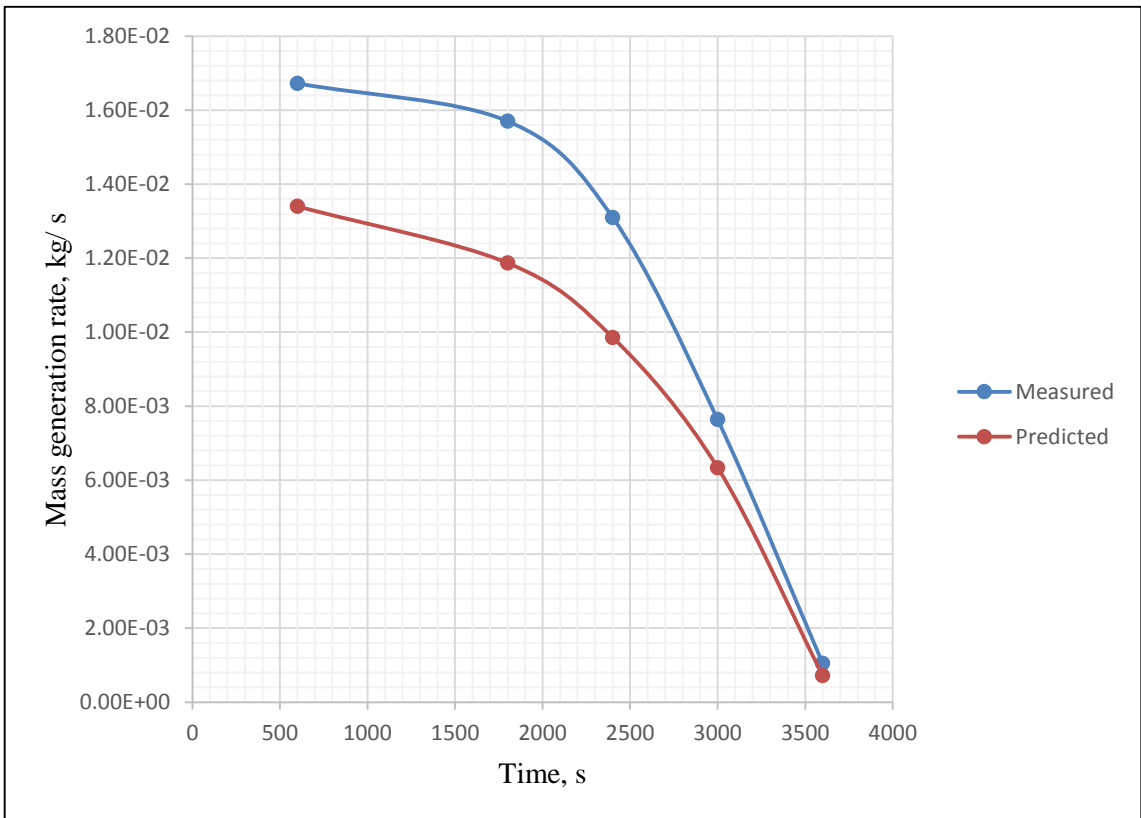


Figure 10: Mass generation rate of methane versus time for Ruan et al. (2012)

Based on Figure 7, Figure 8, Figure 9 and Figure 10, mass generation rate of methane for both calculated and predicted follow the same trend in which it declines with time. As time passes, more hydrates are dissociated into gaseous methane, resulting in lesser methane hydrates in the porous media. This corresponds to the declining pattern of the mass generation rate of methane during the hydrates dissociation. It is also important to note that the calculated mass generation rate exhibits a similar declining pattern to that of the predicted mass generation rate. This is a good indicator that the mathematical model could predict the production of methane from its hydrates dissociation.

The difference between the values of calculated and predicted mass generation rate can also be presented in another form of graph. For the predicted graph line, the values of every x- and y-coordinate are using the value of the predicted mass generation rate itself. This is to ensure that the line can be formed linearly. As for the calculated graph line, the value for x-coordinate is the value of the predicted mass generation rate at a similar time of occurrence, while the y-coordinate is the value of the calculated mass generation rate.

Figure 11, Figure 12, Figure 13 and Figure 14 show the described graphs for Nazridoust and Ahmadi (2007), Kumar et al. (2010), Liu and Gamwo (2012) and Ruan et al. (2012) respectively.

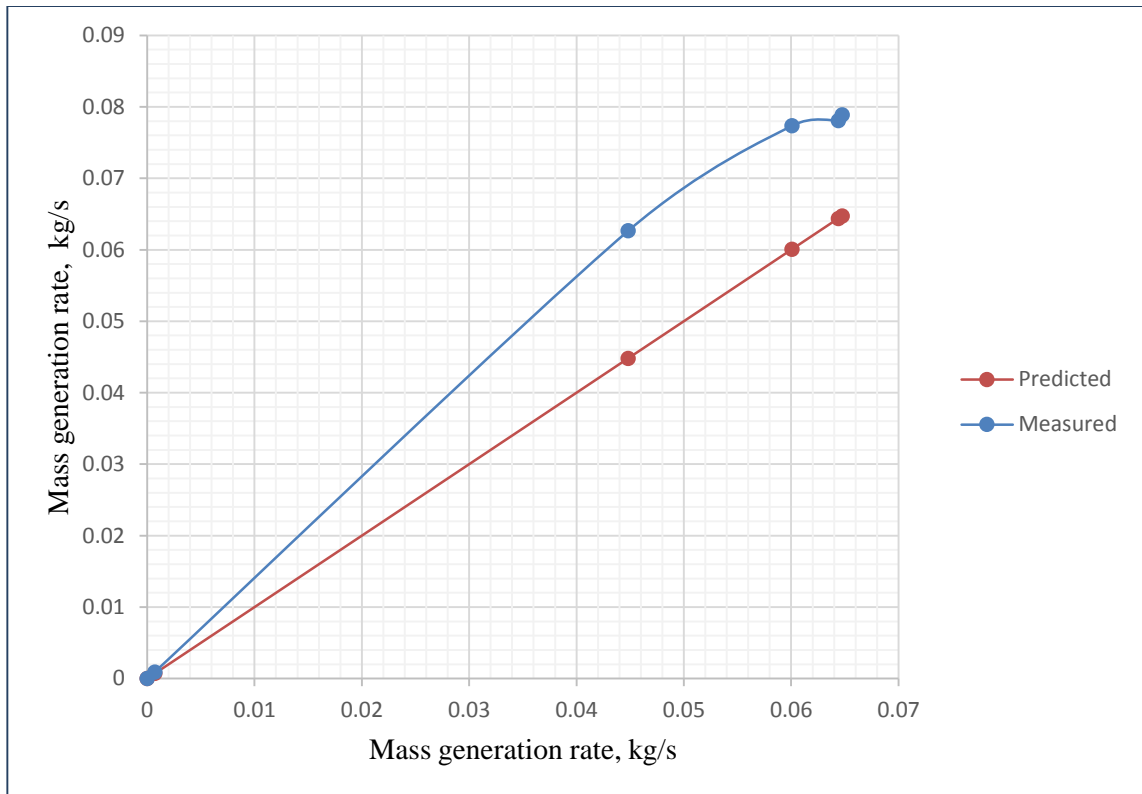


Figure 11: Comparison of mass generation rate for Nazridoust and Ahmadi (2007)

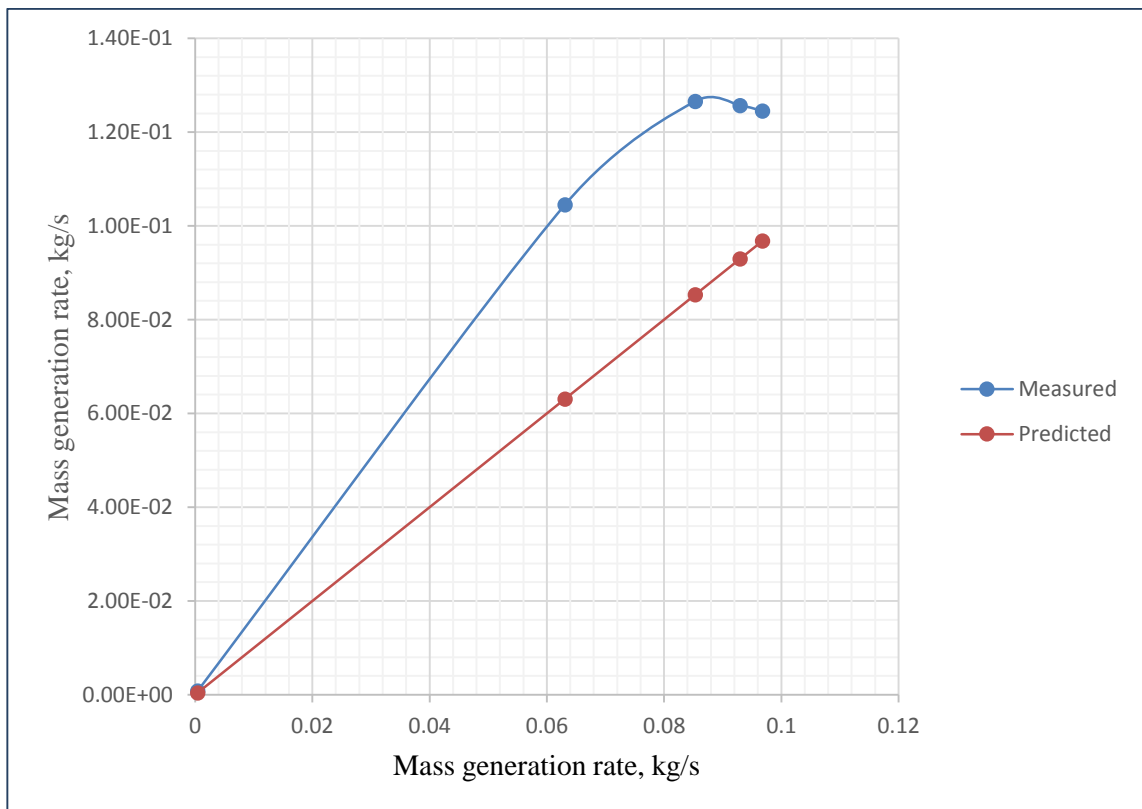


Figure 12: Comparison of mass generation rate for Kumar et al. (2010)

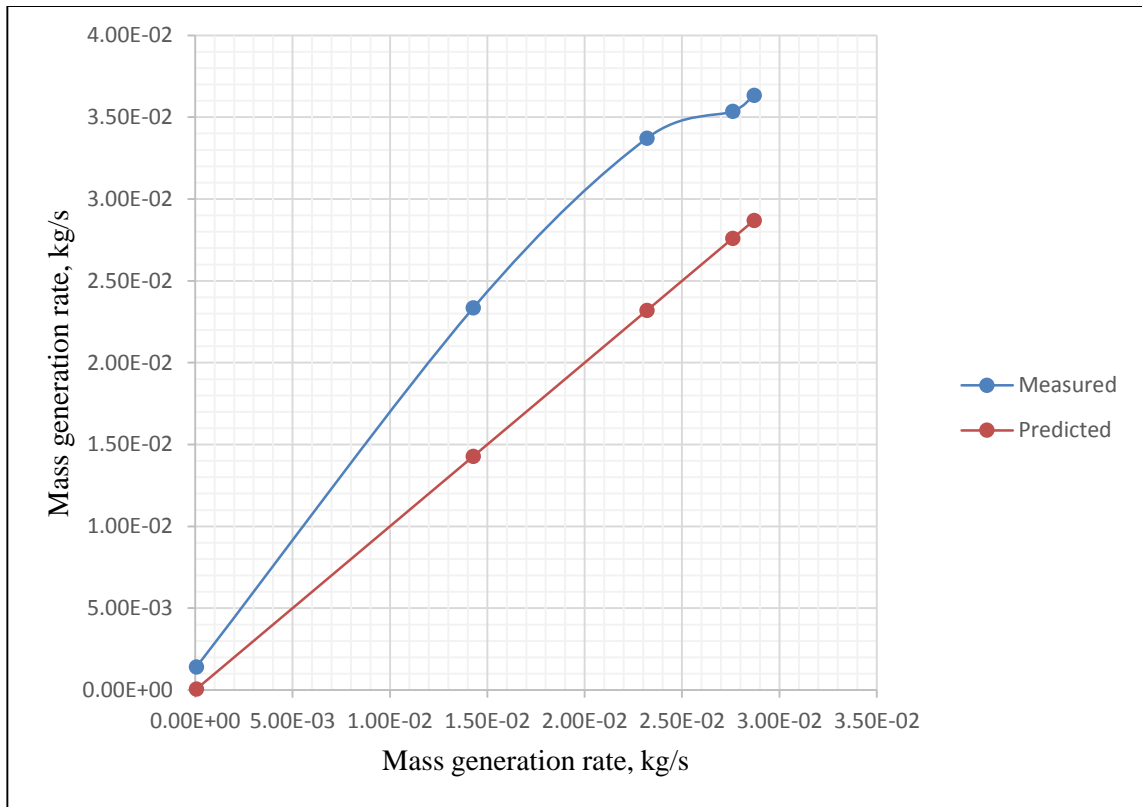


Figure 13: Comparison of mass generation rate for Liu and Gamwo (2012)

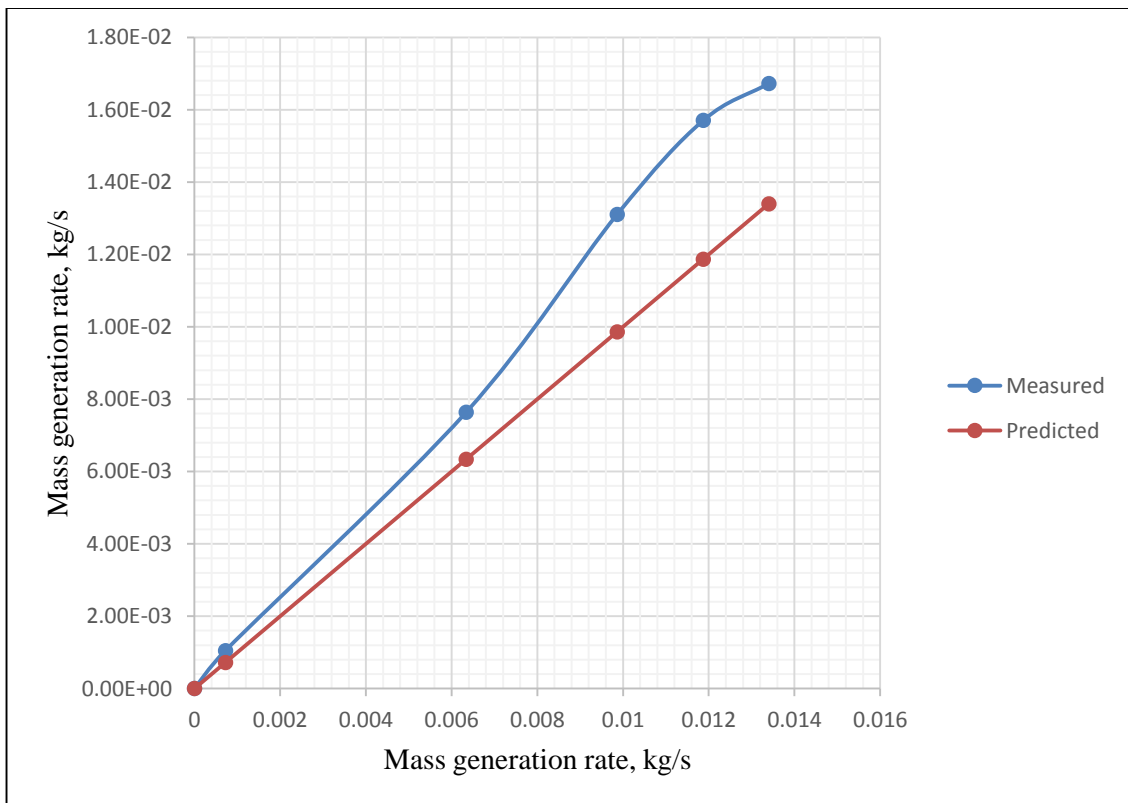


Figure 14: Comparison of mass generation rate for Ruan et al. (2012)

All of the percentage errors are more than 20%. One of the main reasons is the assumptions that have been made in the calculations. Due to insufficient data given in the research papers, some constants such as the intrinsic dissociation rate and activation energy are used in all four cases. It is also assumed that glass beads were used in all four cases in order to calculate the total surface area of hydrates per unit volume. Some research papers use sand core instead of glass beads in their experiment and the difference in the mass, density and radius of the material used may yield significant percentage error. Some research papers do not provide necessary values for the parameter. For instance, in Liu and Gamwo (2012), the values of porosity during the dissociation phase are not given. Thus, the values were assumed in the calculations to fit the expected result, by using the experimental data from other research papers as reference. Another important thing to note is that the formula (equation (12)) used to calculate the area of grain surface area per unit volume of porous media may not be suitable. According to Kumar et al. (2010), for hydrate saturation that is less than 35%, it is assumed that the hydrate formation habit is grain-coating.

In this project, all of the research papers use an initial hydrate saturation of more than 35%. But, since there is not much information as to how to calculate the surface area per unit volume of porous media, this equation is just used for the time being. Apart from that, another two things that may affect the accuracy of the experimental results are the variations in the experiment procedure settings. Due to some human errors while conducting the experiment, the final result of the experiment may be slightly deviated from the original one.

A very important thing to note is that only Kumar et al. (2010) conducted their own experiment and came out with their own results. For other research papers, their experimental data are taken from other researches that have conducted their own experiment, like Masuda et al. (1999). The scarcity of experimental data could be because of the difficulty to set up the experiment itself and the availability of the methane hydrates. Despite the large percentage error, the application of Kim et al. (1987) mathematical model show a promising result as all the measured mass generation rate show similar

declination trend to that of the predicted mass generation rate. The results could have been much improved if more data were given and less assumptions were made.

CHAPTER 5

CONCLUSION AND RECOMMENDATIONS

5.1 Conclusion

The future world needs alternative energy sources to curb for energy crisis and meet the population demands. Today, methane hydrate receives lot of attention due to its potentially large size of untapped resource. A lot of countries have been conducting active researches to extract methane gas efficiently from its hydrate. There are three main methods to assist in dissociation of methane gas from methane hydrate reserves, namely thermal injection, depressurization and inhibitor fluids injection. The objective of this project is to select various mathematical models that simulate the dissociation of methane hydrates in porous media via depressurization and subsequently, to verify the efficiency of the selected mathematical model by testing it with data from various research paper of the same scope of study. Kim et al. (1987) mathematical model is selected as the most ideal model since it is widely referred to and simple. The mathematical model is tested using data from four research papers, namely Nazridoust and Ahmadi (2007), Kumar et al. (2012), Liu and Gamwo (2012) and Ruan et al. (2012). The mass generation rates are calculated and compared to the predicted mass generation rates that are converted from the predicted volume generation rate. When the graph of mass generation rate versus time is plotted, it is found out that the measured mass generation rate declines over time, following a similar pattern like that of the predicted mass generation rate. However, the percentage difference between the two values are quite big with most of them having larger than 20%. The significant percentage error could be contributed by the assumptions made in calculations, insufficient data in the past research papers, and variations in the

experiment procedure and settings and human errors while conducting the experiment. The error could have been largely minimized if more information were given in the research papers and less assumptions were made in calculations. Even so, because the calculated results follow a similar pattern to that of the predicted data, Kim et al. (1987) mathematical model could be the most efficient model to predict the dissociation of methane hydrates in porous media. The objectives are successfully met.

5.2 Recommendations

To improve the quality of the project, the mathematical model should be validated with more research papers that provide the necessary information. Ample time should be allocated to search for such research papers since the research related to methane hydrates is still considered new and so, the source could be scarce. Furthermore, researchers are recommended to conduct the experiment to produce a better predicted or expected data by using the correct experiment procedure and settings. Apart from that, researchers should also spend more time to understand the other mathematical models that have been proposed in other research papers so that the efficiency of Kim et al. (1987) can be compared to the other proposed mathematical models one day.

REFERENCES

- Bailey, A. (2010). *Methane Hydrate: A Future Clean Energy Source?* Retrieved February 11, 2014 from <http://www.greeningofoil.com/post/Methane-hydrate-a-future-clean-energy-source.aspx>.
- Demirbas, A. (Ed.). (2010). *Methane gas hydrate*. Springer.
- Foran, C. (2013). *Is Methane Hydrate the Energy Source of the Future?* Retrieved February 11, 2014 from <http://www.nationaljournal.com/energy/is-methane-hydrate-the-energy-source-of-the-future-20131224>
- Hong, H., Pooladi-Darvish, M. and Bishnoi, P., 2003. Analytical modelling of gas production from hydrates in porous media. *Journal of Canadian Petroleum Technology*, 42(11), pp.45--56.
- Hydrate Dissociation* (n.d.) In National Oceanography Centre. Retrieved February 11, 2014 from <http://noc.ac.uk/science-technology/earth-ocean-system/seafloor/hydrate-dissociation>.
- Konno, Y., Masuda, Y., Oyama, H., Kurihara, M., & Ouchi, H. (2010, January). SS-Gas Hydrate: Numerical Analysis on the Rate-Determining Factors of Depressurization-Induced Gas Production from Methane Hydrate Cores. In *Offshore Technology Conference*. Offshore Technology Conference.
- Kumar, A., Maini, B., Bishnoi, P. R., & Clarke, M. (2013). Investigation of the Variation of the Surface Area of Gas Hydrates during Dissociation by Depressurization in Porous Media. *Energy & Fuels*, 27(10), 5757-5769.
- Kumar, A., Maini, B., Bishnoi, P. R., Clarke, M., Zatsepina, O., & Srinivasan, S. (2010). Experimental determination of permeability in the presence of hydrates and its effect on the dissociation characteristics of gas hydrates in porous media. *Journal*

of Petroleum Science and Engineering, 70(1), 114-122.

- Lee, S. Y., & Holder, G. D. (2001). Methane hydrates potential as a future energy source. *Fuel Processing Technology*, 71(1), 181-186.
- Liang, H., Song, Y., & Chen, Y. (2010). Numerical simulation for laboratory-scale methane hydrate dissociation by depressurization. *Energy Conversion and Management*, 51(10), 1883-1890.
- Liu, Y., & Gamwo, I. K. (2012). Comparison between equilibrium and kinetic models for methane hydrate dissociation. *Chemical Engineering Science*, 69(1), 193-200.
- Lonero, A. (2008). How are Methane Hydrates Formed, Preserved, and Released?. *Hohonu*, 53.
- Mahajan, D., Taylor, C. E., & Mansoori, G. A. (2007). An introduction to natural gas hydrate/clathrate: the major organic carbon reserve of the Earth. *Journal of Petroleum Science and Engineering*, 56(1), 1-8.
- Makogon, Y. F., Holditch, S. A., & Makogon, T. Y. (2007). Natural gas-hydrates—A potential energy source for the 21st Century. *Journal of Petroleum Science and Engineering*, 56(1), 14-31.
- Max, M. D. (Ed.). (2003). *Natural gas hydrate in oceanic and permafrost environments* (Vol. 5). Springer
- Nagao, J. (2012). Development of methane hydrate production method. *Synthesiology English edition*, 5(2), 88-95.
- Nazridoust, K., & Ahmadi, G. (2007). Computational modeling of methane hydrate dissociation in a sandstone core. *Chemical engineering science*, 62(22), 6155-6177.

Pfeifer, S. (2014). *Methane Hydrates Could be Energy of the Future*. Retrieved February 11, 2014 from <http://www.ft.com/intl/cms/s/0/8925cbb4-7157-11e3-8f92-00144feabdc0.html#axzz2tqhbukgY>

Popular Mechanics: Methane Hydrates -- Energy Source of the Future? (2009). Retrieved February 11, 2014 from <http://www.popularmechanics.com/science/environment/2558946>.

Ruan, X., Song, Y., Zhao, J., Liang, H., Yang, M., & Li, Y. (2012). Numerical Simulation of methane production from hydrates induced by different depressurizing approaches. *Energies*, 5(2), 438-458.

Ruan, X., Yang, M., Song, Y., Liang, H., & Li, Y. (2012). Numerical studies of hydrate dissociation and gas production behavior in porous media during depressurization process. *Journal of Natural Gas Chemistry*, 21(4), 381-392.

Ruppel, C. (2011). Methane hydrates and the future of natural gas. *MITEI Natural gas Report, Supplementary Paper on Methane Hydrates*, 4, 25.

Shahbazi, A., & Pooladi-Darvish, M. (2013). Behavior of depressurization in type III hydrate reservoirs. *SPE Journal*, (Preprint).

Steffones, K., Chaturvedi, K. R., & Sihag, P. (2014, January). Fuelling the Future with Gas Hydrates as a Perpetual Energy Source. In *International Petroleum Technology Conference*. International Petroleum Technology Conference.